

Received August 24, 2019, accepted September 10, 2019, date of publication September 20, 2019, date of current version October 2, 2019.

Digital Object Identifier 10.1109/ACCESS.2019.2942633

# A MILP-Based Restoration Technique for Multi-Microgrid Distribution Systems

**MOHEEB OTT<sup>1</sup>, MOHAMMAD ALMUHAINI<sup>ID1</sup>, (Senior Member, IEEE),  
AND MUHAMMAD KHALID<sup>ID1,2</sup>, (Member, IEEE)**

<sup>1</sup>Electrical Engineering Department, King Fahd University of Petroleum and Minerals, Dhahran 31261, Saudi Arabia<sup>2</sup>K.A.CARE Energy Research and Innovation Center, Dhahran 31261, Saudi Arabia

Corresponding author: Mohammad AlMuhaini (muhaini@kfupm.edu.sa)

This work was supported by the Deanship of Research (DSR), King Fahd University of Petroleum and Minerals (KFUPM), under Project IN161043.

**ABSTRACT** The main focus of the work presented in this paper is on the outage management of interconnected microgrids during islanded operation after being disconnected from the utility main supply. The proposed two-stage load restoration technique is formulated as a Mixed Integer Linear Programming (MILP) optimization problem with the sole objective of optimally restoring the maximum number of disconnected loads. The proposed technique is applied to a distribution system comprising of several microgrids, i.e., Multi-Microgrid (MMG) distribution system. In this proposed technique, the power transactions between individual microgrids are managed through (1) determining the schedule of local energy resources, and (2) by obtaining the control signals pertaining to local flexible loads. Flexible load control signals are prioritized through two incorporated Demand Response (DR) programs, namely emergency load shedding and preemptive load shifting. To quantify the restoration technique performance, a new index—denoted as restoration technique success index (SI)—is proposed. The effectiveness of the proposed restoration technique is verified through different test case scenarios and the obtained results are discussed.

**INDEX TERMS** Multi-microgrid, optimization, restoration technique, rolling horizon.

## NOMENCLATURE

$t$	Index of time slot	$C^{CG}$	Cost of conventional DG unit generation
$i$	Index of microgrid	$C^{RG}$	Cost of renewable DG unit generation
$g$	Index of conventional DG unit	$C^{Shed}$	Cost of load shedding
$r$	Index of renewable DG unit	$C^{Ch}$	Cost of ESS charging
$l$	Index of load point	$C^{Dch}$	Cost of ESS discharging
$s$	Index of ESS unit	$DR$	Maximum ramp-down rate of conventional DG
$n$	Index of allowable surplus power utilization interval of conventional DG	$UR$	Maximum ramp-up rate of conventional DG
$N_g$	Number of conventional DG units	$UT$	Minimum up time of conventional DG
$N_r$	Number of renewable DG units	$DT$	Minimum down time of conventional DG
$N_s$	Number of ESS units	$T^{on}$	Duration of period in which conventional DG was ON
$N_l$	Number of load points	$T^{off}$	Duration of period in which conventional DG was OFF
$T_{local}$	Horizon of local scheduling optimization	$X$	Conventional DG unit availability indicator
$T_{shift}$	Horizon of preemptive load shifting signal generation	$P^{Load}$	Demand of load point
$T_{emrg}$	Expected duration of emergency	$\eta^{ch}$	Charging efficiency of ESS
$\Delta t$	Time slot duration	$\eta^{dch}$	Discharging efficiency of EES
		$\tau_{IJ}$	Availability of a tie line between microgrid $i$ and microgrid $j$
		$T_{ij}^{max}$	Maximum capacity of a tie line between microgrid $i$ and microgrid $j$

The associate editor coordinating the review of this manuscript and approving it for publication was Giacomo Verticale<sup>ID</sup>.

$e$	Emergency starting time
$P^{CG}$	Conventional DG generation
$I$	Conventional DG commitment indicator
$X$	Conventional DG availability indicator
$u$	Conventional DG start-up indicator
$d$	Conventional DG shutdown indicator
$P^{RG}$	Renewable DG generation
$P^{Shed}$	Amount of load shedding (local scheduling)
$P^{Ch}$	Power charging rate of ESS
$P^{Dch}$	Power discharging rate of ESS
$ch$	ESS charging indicator
$dch$	ESS unit discharging indicator
$CG$	Utilized surplus power from conventional DG
$Z$	Interval indicator of utilized surplus power from conventional DGs
$RG$	Utilized surplus power from renewable DG
$ES$	Utilized surplus power from ESS
$T_{ij,t}^+$	Power transferred to microgrid $i$ from microgrid $j$
$T_{ij,t}^-$	Power transferred from microgrid $i$ to microgrid $j$
$LS$	Amount of load shedding (global scheduling)
$adj$	Adjustable power (surplus power)
$I$	Optimal value after local scheduling
$II$	vOptimal value after global scheduling
$LP$	Low Priority
$MP$	Medium Priority
$HP$	High Priority

## I. INTRODUCTION

With the rapid development of modern industry and the increasing electrification of civilized societies, the reliance on and the demand for electrical power is increasing [1]. As a result, the impact of any outage, especially catastrophic outages, is becoming more severe than before. Available evidence indicates that the number and cost of such power outages are highly significant. For example, according to the data published in a report from North American Electric Reliability Corporation (NERC), 80% of all outages in the U.S. that occurred between 2003 and 2012 were weather-driven, causing around 147 million customers to lose their power supply for at least one hour [2]. Moreover, statistics provided by the U.S. Department of Energy (DOE) indicate that weather-driven sustained service interruptions in the United States cost on average US\$18 to US\$33 billion per year [3]. Considering the above-mentioned arguments and the fact that the frequency and strength of natural disasters is expected to increase [4], as is power consumption, enhancing the system resiliency and reliability is more crucial than ever. On the system level, resiliency can be improved by strengthening the infrastructure or improving the recovery and survival abilities of the power system [5]. Any beneficial change in the design, the construction guidelines, or the characteristics and features of the system components is considered infrastructure improvement. Increasing the number of the underground

cables, moving the feeders into safer paths, and deploying transmission towers and poles of better quality are some examples of power system infrastructure strengthening.

The aim of this work is enhancing the outage recovery and survivability of the power system by proposing a smart load restoration technique. The restoration technique is designed and applied to Multi-Microgrid (MMG) distribution systems working in islanded operation mode following contingencies. In the present context, recovery and survivability can be defined as the capacity of islanded microgrids to continue at or near the level of normal functioning without the need for full power support from the main grid.

Microgrid, as a source of resiliency and operational support to the power system, has been studied extensively in the pertinent literature. The feasibility of a microgrid to serve as a resiliency source is studied in [6]. Three configurations of microgrid deployment as resiliency source were considered, namely as a local source, community source, and black start source. Microgrids deployed as local resources operate to ensure a continuous interruptible power service for local consumers within their boundaries. When acting as a community resource, microgrids utilize their unused resources to restore interrupted loads outside their boundaries, thereby enhancing the resiliency of the entire system.

Microgrids serving as a black start resource are intended to assist in the black start of main generation units comprising the main grid. In [7] and [8], microgrids are used to support resiliency of the main grid by participating in restoration of interrupted loads outside their boundaries. A multi-level load restoration scheme is proposed in [7], where generation capabilities of microgrids and Electric Vehicles (EVs) are used to enhance system reliability and resiliency after contingencies. In [8], a resiliency-based service restoration approach aimed at managing catastrophic outages caused by main disasters is suggested. Moreover, the dynamic performance of a distributed generation and microgrid stability is considered. Limits on frequency deviation, transient currents, and voltages are incorporated as constraints. Gouveia and colleagues [9] focused on constructing management functionalities to manage Energy Storage System (ESS) charging and discharging processes in microgrids, and to send controlling signals for responsive loads, including EVs. The main objective was to enhance microgrid resiliency following an islanding event. A resiliency-based microgrid operational control framework is proposed in [10] with an objective of enhancing resiliency by minimizing load curtailment after contingencies. Both grid-connected and islanded operations are considered. The grid-connected operation is modeled as a Mixed Integer Linear Programming (MILP) problem, while islanded mode is modeled as a linear programming problem. The uncertainty inherent in renewable generation resources and loads is considered by using robust optimization strategies.

Adjustable loads with predefined start and end times are adopted in load modeling. In [11], the authors focused on utilizing demand-side management to restore a microgrid during an outage. They proposed a demand management

mechanism whereby the loads were classified into interruptible and critical categories. The behavior of the microgrid during the outage is reflected by a proposed new metric “grid autonomy factor.” An energy management system for enhancing the resiliency of microgrids in islanded operation is proposed in [12]. A stochastic nonlinear programming optimization problem is formulated by the authors with the objective of minimizing the number of unserved loads, which are categorized based on priority into critical and non-critical classes. The uncertainty in the renewable resources’ output power is explicitly considered and the demand response is achieved through adjustable loads and PHEVs.

According to the IEEE Standard 1547.4 [13], splitting the power distribution system into interconnected microgrids can improve its resiliency and operation. Researchers, considering both structure and operation, have studied microgrid networking—as an upgraded microgrid form and a more beneficial way to enhance the power system resiliency during contingencies. Goyal and Ghosh [14], for example, investigated support provided by two connected islanded microgrids during contingencies. In this work, microgrids were connected through back-to-back converter, whereby each microgrid supplies its local loads autonomously. When an overloading is detected in one of the microgrids, the other offers power support. Transformative architecture is proposed in [15], where microgrids that are unable to fully supply their local load broadcast supply support requests to other normally operating microgrids. The power transactions from normally operating microgrids to those experiencing emergencies are controlled through a devised average consensus algorithm in a decentralized manner. Privacy-preserving energy management algorithm for a networked microgrid system operating in both islanded and grid-connected modes is introduced in [16], whereby microgrids are nested to inner and outer levels based on load priorities. System resiliency enhancement is the main objective in islanded operation, and is achieved by enabling disconnected microgrids to form subgroups [17]–[19]. In [20], the authors proposed an outage restoration technique for power systems after natural disasters. The grid is sectionalized into self-adequate multiple microgrids, which are coordinated to restore critical loads by formulating an MILP optimization problem.

A comprehensive review of pertinent literature suggests that the response of multi-microgrid systems in order to survive catastrophic outage should be studied further, with a particular focus on the means of coordinating local resources and applying suitable demand response programs. These issues are addressed in this work and its main contributions can be summarized as follows:

- A novel two-stage restoration technique is proposed to supply and restore disconnected loads during outages. Two Demand Response (DR) programs are incorporated into the proposed restoration technique, namely pre-emptive load shifting and emergency load shedding programs. The stages of the proposed technique are formulated as an MILP optimization problem, which

can be easily implemented and solved by available commercial solvers, such as CPLEX [21].

- A new index, restoration technique, Success Index (SI), is proposed to reflect the performance of the proposed technique. The index is calculated by comparing the system’s survival capability before and after applying the technique.

## II. PROBLEM AND SYSTEM DISCRIPTION

The main objective of this work is to propose a load restoration technique that can be applied to MMG distribution systems islanded from the main grid after contingencies. Each microgrid is connected to the remainder of the distribution system through the Point of Common Coupling (PCC) and comprises of multiple conventional and renewable Distributed Generators (DGs), Energy Storage System (ESS), and controllable and non-controllable loads, as shown in Figure 1.

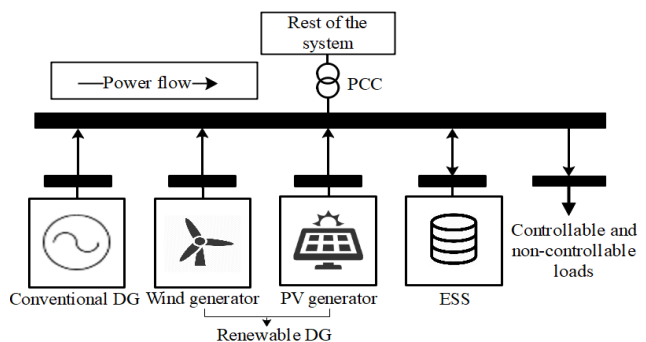


**FIGURE 1.** Microgrid schematic.

Three factors are considered as the primary drivers for deployment of DSM actions: energy efficiency (EE), energy conservation (EC) and demand response (DR). DR denotes direct control of (specific types of) electrical equipment, typically aimed at reducing system peak load, or as a part of network balancing mechanism, or to realize certain system support capabilities, or to provide different types of system reserve. Typically, DSM activities are based on the electricity market and price or tariff signals that are sent to customers by utilizing Advanced Metering Interface (AMI). In this context, the term “controllable loads” refers to the loads that can be shed or shifted if required by applying DR. In this study, it is assumed that there is no mismatch between the scheduled load shedding/shifting and the actual controlled load.

A hierarchical operational and control framework consisting of three levels of control is proposed. In the control framework, lower-level control agents receive commands from the upper levels, yet the latter base their decisions on the data collected from the lower-level control agents.

The first control level is the lowest level, consisting of two control agent types, namely local microsource controller (MC) and local load controller (LC). The second control level consists of one control agent, the microgrid controller (MGC). Finally, the third control level is the highest

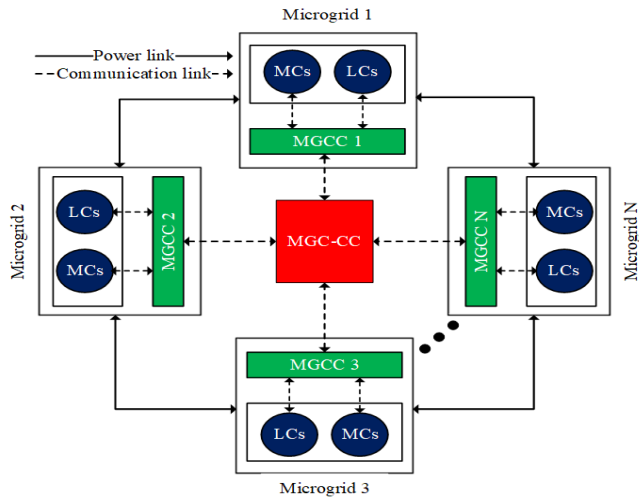


**FIGURE 2.** Proposed MMG system control and operational framework.

level, otherwise known as the microgrid community central controller (MGC-CC). The proposed operational and control framework of the MMG distribution system is depicted in Figure 2. The rules and responsibilities of each control agent are summarized below.

- A. Level I (MC and LC): LCs are mainly responsible for setting the on/off state of the associated load points, based on the command signals produced by the MGC. MCs, on the other hand, are responsible for ensuring that the generation power is supplied by the DGs locally installed in the microgrid (as scheduled by the MGC), while keeping the voltage and frequency of the microgrid within acceptable limits.
- B. Level II (MGC): MGC is responsible for scheduling the local resources and microgrid loads, as well as producing control signals to Level I controllers. Scheduling is based on the forecasted demand and supply computed locally in the MGC controller. Additionally, MGC collects data pertaining to the power deficit or surplus within the microgrid to be sent to the MGC-CC.
- C. Level III (MGC-CC): MGC-CC is responsible for optimizing the power transactions between microgrids comprising the MMG system. Power transactions are determined by the data received from MGCs. Once all power transactions are determined, MGC-CC sends signals to MGCs to update the generation schedule.

### III. PROPOSED RESTORATION TECHNIQUE

#### A. RESTORATION TECHNIQUE STAGES

The proposed load restoration technique is designed for the application on the islanded MMG system after contingencies at the utility side. It consists of two stages, both of which are formulated as an MILP optimization problem. In the first stage, the pre-emptive load shifting DR program is applied to reshape the load profile depending on available resources. In the second stage, available resources are scheduled in two steps, whereby scheduling of local microgrids' resources and controllable loads is followed by the determination of

power transactions. The MMG distribution system is assumed to operate in islanding mode during emergencies and the internal components in each microgrid in the system are 100% reliable. The restoration technique stages are illustrated below.

- A. First Stage (Pre-emptive Load Shifting DR Program) Once an emergency is detected, MGC associated with each microgrid generates load shifting signals for the next  $T_{shift}$  time steps, considering the forecasted demand and supply data  $F$  and the technical constraints imposed on the system components. These signals are sent to the corresponding LCs, and are subsequently relayed to the customers.
- B. Second Stage (Local and Global Scheduling) In the first step of the second stage, each microgrid's MGC schedules the available local resources and determines the amount of the emergency load shedding necessary based on the data it receives from local LCs and MCs. This is done by solving the MILP Rolling Horizon (RH) optimization framework problem wherein, at each slot, the MGC schedules the local resources and controllable loads for a specific period of time (local optimization scheduling horizon,  $T_{local}$ ). However, only the schedule for the following time slot is performed next (denoted as local optimization scheduling control horizon). Once the schedule of resources and controllable load is determined, the MGCs calculate the surplus and deficit energy for the next time slot within every microgrid and report the data to the MGC-CC.

The main advantage of the RH optimization strategy is the outcome control for a particular time slot, while considering its successors and maintaining the ability to respond to unforeseen events. Therefore, this strategy provides further flexibility for the proposed load restoration technique. In addition, by adopting the RH optimization strategy, the robustness of the proposed technique increases, as it implicitly tolerates the volatility of the renewable generation. Figure 3 depicts the RH optimization strategy, distinguishing between scheduling and control horizons.

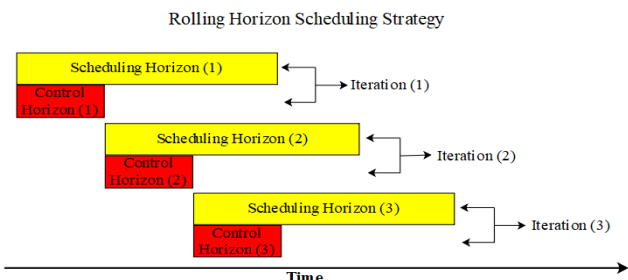


**FIGURE 3.** Rolling horizon scheduling strategy operation.

In the next step of the second stage, MGC-CC schedules the power transactions between the microgrids for the subsequent time slot based on the information sent by the MGCs. Next, both the updated set points for the generation

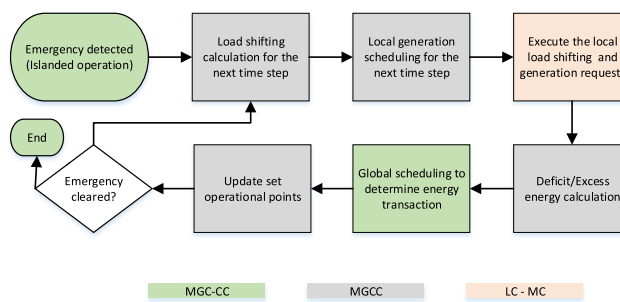


**FIGURE 4.** Proposed load restoration technique flow chart.

of DGs and the load shedding signal for the current time step are sent to MGCS and corresponding MCs and LCs, respectively, which respond accordingly. At the end of each time step, the MGCC checks whether the system emergency is cleared. If the system emergency status is still activated, the next time slot is scheduled; otherwise, the load restoration technique is terminated. Figure 4 summarizes the stages of the proposed restoration technique and the rules imposed on the control agents.

The next three subsections are designated for the mathematical formulation of the preemptive load shifting signal generation, local scheduling, and global scheduling optimization problems. However, although the preemptive load shifting DR program is the first step taken once an emergency is detected, local and global scheduling formulation is presented beforehand for convenience.

### B. OPTIMIZATION OF MICROGRID LOCAL SCHEDULING

The RH optimization strategy was adopted at this stage. It was performed over several time steps,  $T_{Local}$ , wherein the cost function of all the periods was minimized. However, only the scheduling of the next time step is considered. The local scheduling optimization problem is formulated as follows:

$$\min \sum_{t=e}^{e+T_{Local}-1} \left\{ \sum_{g=1}^{N_g} C_{g,i}^{CG} P_{g,i,t}^{CG} + \sum_{r=1}^{N_r} C_{r,i}^{RG} P_{r,i,t}^{RG} + \sum_{l=1}^{N_l} C_{l,i}^{Shed} P_{l,i,t}^{Shed} + \sum_{s=1}^{N_s} C_{s,i}^{Ch} P_{s,i,t}^{Ch} + \sum_{s=1}^{N_s} C_{s,i}^{Dch} P_{s,i,t}^{Dch} \right\} \Delta t \quad (1)$$

The main aim of the objective function given by (1) is to supply the maximum load to each microgrid at a minimum cost in  $T_{Local}$  time steps subject to the following constraints:

Power balance,

$$\sum_{g=1}^{N_g} P_{g,i,t}^{CG} + \sum_{r=1}^{N_r} P_{r,i,t}^{RG} + \sum_{l=1}^{N_l} P_{l,i,t}^{Shed} + \sum_{s=1}^{N_s} P_{s,i,t}^{Dch} = \sum_{l=1}^{N_l} P_{l,i,t}^{Load} + \sum_{s=1}^{N_s} P_{s,i,t}^{Ch} \quad (2)$$

Conventional DGs power output limit,

$$I_{g,i,t} X_{g,i,t} P_{g,i}^{CG,min} \leq P_{g,i,t}^{CG} \leq I_{g,i,t} X_{g,i,t} P_{g,i}^{CG,max} \quad (3)$$

Conventional DGs maximum up/down rates,

$$P_{g,i,t-1}^{CG} - P_{g,i,t}^{CG} \leq DR_{g,i} (1 - d_{g,i,t}) + P_{g,i}^{CG,max} d_{g,i,t} \quad (4)$$

$$P_{g,i,t}^{CG} - P_{g,i,t-1}^{CG} \leq UR_{g,i} (1 - u_{g,i,t}) + P_{g,i}^{CG,max} u_{g,i,t} \quad (5)$$

Conventional DGs minimum up/down times,

$$\sum_{t=t}^{t+UT_{g,i}-1} I_{g,i,t} \geq UT_{g,i} u_{g,i,t} \quad (6)$$

$$\sum_{t=t}^{t+DT_{g,i}-1} (1 - I_{i,t}) \geq DT_{g,i} d_{g,i,t} \quad (7)$$

Equations (4-7) depend on the start-up and shutdown indicators that are calculated based on the commitment indicators, as shown in (8) and (9).

$$u_{g,i,t} - d_{g,i,t} = I_{g,i,t} - I_{g,i,t-1} \quad (8)$$

$$u_{g,i,t} + d_{g,i,t} = 1 \quad (9)$$

ESS maximum charge rate,

$$0 \leq P_{s,i,t}^{Ch} \leq ch_{s,i,t} P_{s,i}^{Ch,max} \quad (10)$$

ESS maximum discharge rate,

$$0 \leq P_{s,i,t}^{Dch} \leq dch_{s,i,t} P_{s,i}^{Dch,max} \quad (11)$$

ESS energy level,

$$SOC_{s,i}^{min} \leq SOC_{s,i,t} \leq SOC_{s,i}^{max} \quad (12)$$

Equation (13) aims to prevent simultaneous charging and discharging of the same ESS unit.

$$dch_{s,i,t} + ch_{s,i,t} = 1 \quad (13)$$

The relationship that the charged or discharged power has with the SOC of the ESS unit is modeled by,

$$SOC_{s,i,t+1} = SOC_{s,i,t} + \left( \frac{\left( \eta_{s,i}^{ch} P_{s,i,t}^{ch} - \frac{P_{s,i,t}^{dch}}{\eta_{s,i}^{dch}} \right) \Delta t}{C_{s,i}^{ESS}} \right) \quad (14)$$

Finally, (15) and (16) set the limits on the utilized renewable generation and the load shedding amount at each load point, respectively.

$$0 \leq P_{r,i,t}^{RG} \leq P_{r,i,t}^{RG,max} \quad (15)$$

$$0 \leq P_{l,i,t}^{Shed} \leq P_{l,i,t}^{Load} \quad (16)$$

Once local scheduling is completed, MGCS calculate the surplus and deficit power in each microgrid and send this data to the MGCC to optimize power transactions between microgrids. This data is calculated as follows:

- I. Deficit microgrid power: calculated by summing the load shedding determined in local scheduling as shown below:

$$P_{i,t}^{Deficit} = \sum_{l=1}^{N_l} (P_{l,i,t}^{Shed,I}) \quad (17)$$

- II. Maximum adjustable power of microgrid's local renewable generators: equal to the sum of the unutilized generation of each renewable DG unit in local scheduling, as shown below:

$$P_{i,t}^{max-adj,RG} = \sum_{r=1}^{N_r} (P_{r,i,t}^{RG,max} - P_{r,i,t}^{RG,I}) \quad (18)$$

III. Maximum adjustable power of microgrid's local ESS units: determined by first calculating the maximum adjustable power of all ESS units (18–20)

$$C = E_{s,i,t+T_{local}} - E_{s,i}^{min} \quad (19)$$

$$D = E_{s,i,t} - E_{s,i}^{min} \quad (20)$$

$$\begin{aligned} P_{s,i,t}^{adj,ESS} &= \begin{cases} \min \left\{ \frac{\min(C, D - \frac{P_{s,i,t}^{Dch,I}}{\eta_{s,i}^{dch}}) *}{\Delta t}, \left( P_{s,i}^{Dch,max} - P_{s,i,t}^{Dch,i} \right) \right\}, \\ \qquad \qquad \qquad dch_{s,i,t} = 1 \\ \min \left\{ \frac{\min(C, D + P_{s,i,t}^{Ch,i} \eta_{s,i}^{ch}) * \eta_{s,i}^{dch}}{\Delta t}, \left( P_{s,i}^{Dch,max} + P_{s,i,t}^{Ch,i} \right) \right\}, \\ \qquad \qquad \qquad ch_{s,i,t} = 1 \\ \min \left\{ \frac{\min(C, D) * \eta_{s,i}^{dch}}{\Delta t}, \left( P_{s,i}^{Dch,max} \right) \right\}, \quad \text{Otherwise} \end{cases} \quad (21) \end{aligned}$$

then calculating the sum of these values (22).

$$P_{i,t}^{max-adj,ESS} = \sum_{g=1}^{N_g} (P_{s,i,t}^{adj,ESS}) \quad (22)$$

It is assumed that only the energy remaining in the next  $(T_{local} + 1)^{th}$  time step is offered as excess energy. This strategy serves as a backup in case that a microgrid is disconnected from the others and has to work autonomously.

IV. Adjustable power of microgrid's conventional generators: calculated by first determining the maximum (22–24) and minimum (26) adjustable power of each unit.

$$E = P_{g,i,t}^{CG,max} - P_{g,i,t}^{CG,i} \quad (23)$$

$$F = P_{g,i,t-1}^{CG,ii} + UR_{g,i} - P_{g,i,t}^{CG,i} \quad (24)$$

$$\begin{aligned} P_{g,i,t}^{adj,CG,max} &= \begin{cases} \min(E, F), \quad I_{g,i,t-1}^{ii} = 1 \\ E, \quad T_{g,i,t}^{off} - DT_{g,i,t} \geq 0 \text{ and } I_{g,i,t-1}^{ii} = 0 \\ 0, \quad \text{Otherwise} \end{cases} \quad (25) \end{aligned}$$

$$\begin{aligned} P_{g,i,t}^{adj,CG,min} &= \begin{cases} 0, \quad I_{g,i,t}^i = 1 \\ P_{g,i}^{CG,min}, \quad T_{g,i,t}^{off} - DT_{g,i,t} \geq 0, I_{g,i,t-1}^{ii} = 0 \text{ and } I_{g,i,t}^i = 0 \end{cases} \quad (26) \end{aligned}$$

These values mainly depend on the commitment state and the up-ramp constraint of the conventional generator unit. To determine the levels of allowable energy participation

of conventional DGs in a certain microgrid, a matrix  $C$  of  $2^{N_g} \times N_g$  dimensions is defined. The elements of matrix  $C$  provide all utilization possibilities of the conventional DGs installed in the microgrid. For example, matrix  $C$  for a microgrid with  $N_g = 2$  has the following form:

$$C = \begin{bmatrix} 1 & 1 \\ 1 & 0 \\ 0 & 1 \\ 0 & 0 \end{bmatrix} = \begin{bmatrix} c_{1,1} & c_{1,2} \\ c_{2,1} & c_{2,2} \\ c_{3,1} & c_{3,2} \\ c_{4,1} & c_{4,2} \end{bmatrix}$$

For  $N_g$  conventional DGs,  $2^{N_g}$  allowable surplus energy ranges are calculated to be sent to the MGC-CC. The boundaries of each interval are calculated as follows:

$$\begin{bmatrix} P_{i,1}^{max-adj,C} P_{i,1}^{min-adj,C} \\ P_{i,2}^{max-adj,C} P_{i,2}^{min-adj,C} \\ \vdots \\ P_{i,2^{N_g}}^{max-adj,C} P_{i,2}^{min-adj,C} \end{bmatrix} = C \times \begin{bmatrix} P_{1,i,t}^{adj,C,max} P_{1,i,t}^{adj,C,min} \\ P_{2,i,t}^{adj,C,max} P_{2,i,t}^{adj,C,min} \\ \vdots \\ P_{N_g,i,t}^{adj,C,max} P_{N_g,i,t}^{adj,C,min} \end{bmatrix} \quad (27)$$

The amount of the utilized surplus from conventional DGs within the microgrid based on the global scheduling must have a value that belongs to one these generation ranges.

### C. OPTIMIZATION OF MICROGRIDS' GLOBAL SCHEDULING

Once the data pertaining to the surplus or deficit power of each microgrid is received, MGC-CC runs an optimization problem to manage the power transactions between the connected microgrids. Global scheduling problem is modeled as follows:

$$\begin{aligned} \min \left\{ \left( \sum_{i=1}^{N_g} C_i^{CG,*} CG_{i,t} + \sum_{i=1}^{N_g} C_i^{RG,*} RG_{i,t} \right. \right. \\ \left. \left. + \sum_{i=1}^{N_g} C_i^{ESS,*} ES_{i,t} + \sum_{i=1}^{N_g} C_i^{Shed*} LS_{i,t} \right. \right. \\ \left. \left. + \sum_{i=1}^{N_g} \sum_{j=i+1}^{N_g} C_{i,j}^{Trans} (T_{ij,t}^+ + T_{ij,t}^-) \right) * \Delta t \right\} \quad (28) \end{aligned}$$

The aim of the objective function (28) is to maximize restoration of loads that were shed as a part of local scheduling while minimizing the cost.

In the model, power balance in each microgrid  $i$  is sustained by (29).

$$CG_{i,t} + RG_{i,t} + ES_{i,t} + LS_{i,t} + \sum_{i=1}^{N_g} \sum_{j \neq i}^{N_g} (T_{ij,t}^+ - T_{ij,t}^-) = L_{i,t} \quad (29)$$

In addition, the required load supply, as determined by the global scheduling, is set to equal the load curtailed in the local scheduling by (30), while (31) ensures that load shedding does not exceed the load.

$$L_{i,t} = P_{i,t}^{Deficit} \quad (30)$$

$$0 \leq LS_{i,t} \leq L_{i,t} \quad (31)$$

Finally, the limits imposed on the utilized surplus power from different resources are given by (31–36).

$$0 \leq RG_{i,t} \leq P_{i,t}^{\max-\text{adj},RG} \quad (32)$$

$$0 \leq ES_{i,t} \leq P_{i,t}^{\max-\text{adj},ESS} \quad (33)$$

$$0 \leq T_{ij,t}^+ \leq \tau_{ij} T_{ij}^{\max} i \neq j \quad (34)$$

$$0 \leq T_{ij,t}^- \leq \tau_{ij} T_{ij}^{\max} i \neq j \quad (35)$$

$$\sum_{n=1}^{2^{N_g}} (P_{i,n}^{\min-\text{adj},CG} Z_n) \leq CG_{i,t} \leq \sum_{n=1}^{2^{N_g}} (P_{i,n}^{\max-\text{adj},CG} Z_n) \quad (36)$$

$$\sum_{n=1}^{2^{N_g}} Z_n = 1 \quad (37)$$

Once MGC-CC determines the power transactions and the amount of utilized power from different resources comprising each microgrid, it notifies the corresponding MGCS to reschedule their respective set points accordingly.

#### D. GENERATION OF PREEMPTIVE LOAD SHIFTING SIGNALS

The main objective of this step is to revise the load profile in accordance with resource (mainly renewable DGs) availability, and to support the restoration of high-priority loads. This is achieved by formulating an optimization problem akin to the local scheduling problem, except that some loads can be shifted. The optimization problem extends to  $T_{shift}$  time steps.  $T_{shift}$  should be set to a value convenient for the participating customers and should not exceed the expected emergency duration. The load shifting signal generation optimization problem is formulated as follows:

$$\begin{aligned} \min \sum_{t=e}^{e+T_{shift}-1} & \left\{ \left( \sum_{g=1}^{N_g} C_{g,i}^{CG} P_{g,i,t}^{CG} + \sum_{r=1}^{N_r} C_{r,i}^{RG} P_{r,i,t}^{RG} \right. \right. \\ & + \sum_{l=1}^{N_l} C_{l,i}^{Shed} P_{l,i,t}^{Shed} + \sum_{s=1}^{N_s} C_{s,i}^{Ch} P_{s,i,t}^{Ch} \\ & \left. \left. + \sum_{s=1}^{N_s} C_{s,i}^{Dch} P_{s,i,t}^{Dch} \right) \Delta t \right\} \\ & + \sum_{t=e}^{e+T_{emrg}-1} \sum_{t'=e, t' \neq t}^{e+T_{shift}-1} C_{t,t'}^{shift} P_{t,t'}^{Shift} \Delta t \end{aligned} \quad (38)$$

The objective function (38) is similar to the one used in the formulation of the local scheduling problem, with the exception of the sixth term, which is added to represent the cost of load shifting. The power balance constraint (39) is also similar to the one used in local scheduling, but load shifting from the microgrid is added as a source, while load shifted to the microgrid is added as a load.

$$\begin{aligned} \sum_{t'=e, t' \neq t}^{e+T_{emrg}-1} P_{i,(t',t)}^{shift} + \sum_{g=1}^{N_g} P_{g,i,t}^{CG} + \sum_{r=1}^{N_r} P_{r,i,t}^{RG} \\ + \sum_{l=1}^{N_l} P_{l,i,t}^{Shed} + \sum_{l=1}^{N_l} P_{s,i,t}^{Dch} = \sum_{l=1}^{N_l} P_{l,i,t}^{Load} \\ + \sum_{l=1}^{N_s} P_{s,i,t}^{Ch} + \sum_{t'=e, t' \neq t}^{e+T_{emrg}-1} P_{i,(t,t')}^{shift} \end{aligned} \quad (39)$$

$$\sum_{t'=e, t' \neq t}^{e+T_{shift}-1} P_{i,(t,t')}^{shift} \leq IF_{i,t} \quad (40)$$

$$\sum_{t'=e, t' \neq t}^{e+T_{shift}-1} P_{i,(t',t)}^{shift} \leq OF_{i,t} \quad (41)$$

Finally, technical constraints (3–16) are also considered.

#### E. LOAD RESTORATION TECHNIQUE – SUCCESS INDEX

To evaluate the performance of the proposed load restoration technique, a Success Index (SI) is proposed. The performance of the proposed technique is assessed relative to the load restoration performance of microgrids working autonomously in islanded mode (non-cooperative operation mode). The proposed SI is calculated as a ratio of the scaled amount of restored load when the proposed technique is applied and that when it is not applied:

$$SI = \frac{\sum_{i=1}^{Ni} \sum_{t=e}^{e+T_{DE}-1} \sum_{l=1}^{Nl} S_{i,l} * (P_{l,i,t}^{Load} - LS_{i,l,t}) \Delta t}{\sum_{i=1}^{Ni} \sum_{t=e}^{e+T_{DE}-1} \sum_{l=1}^{Nl} S_{i,l} * (P_{l,i,t}^{Load} - P_{l,i,t}^{Shed}) \Delta t} \quad (42)$$

where  $T_{DE}$  is the actual duration of emergency and  $S$  is a scaling factor dependent on load point priorities, as shown in Table 1.

**TABLE 1.** Units for magnetic properties.

$S_{l,i}^{HP}$	$S_{l,i}^{MP}$	$S_{l,i}^{LP}$
1.2	1	0.8

#### IV. INPUT DATA AND THE TEST SYSTEM

The distribution system comprising of three microgrids shown in Figure 5 is considered as the test system. In normal conditions, the system operates in a radial energy delivery configuration. In this configuration, the utility grid and local resources only supply microgrid demand.

Once a contingency at the utility side is detected, the system isolates itself through the normally closed breaker and adopts a networked configuration through the normally opened breaker. The technical specifications of the considered wind turbine and PV module are given in [22] and [23], respectively. In the wind generator modeling, the wind turbine generation characteristics are fitted using cubic spline interpolation. For the break points of wind speed and output power provided, the manufacturer formulated nine third-order polynomials for power curve fitting. The coefficients of the cubic spline polynomials are summarized in Table 2.

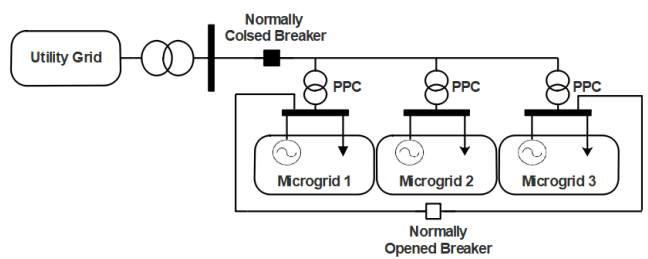


**FIGURE 5.** Test system.

**TABLE 2.** Coefficient of cubic spline polynomials.

<b>n</b>	<b>a<sub>n</sub></b>	<b>b<sub>n</sub></b>	<b>c<sub>n</sub></b>	<b>d<sub>n</sub></b>	<b>Speed Bounds</b>
<b>1</b>	-4354.5	2145.9	0	0	$v \in (2.8,3]$
<b>2</b>	214	-466.82	335.82	51	$v \in (3,4]$
<b>3</b>	-56.369	175.19	44.184	134	$v \in (4,5]$
<b>4</b>	34.474	6.0787	22.45	297	$v \in (5,6]$
<b>5</b>	-13.526	109.5	341.03	563	$v \in (6,7]$
<b>6</b>	-19.369	68.921	519.45	1000	$v \in (7,8]$
<b>7</b>	54.001	10.815	599.18	1569	$v \in (8,9]$
<b>8</b>	-124.64	172.82	782.82	2233	$v \in (9,10]$
<b>9</b>	-117.45	-201.09	754.55	3064	$v \in [10,11]$

The specifications of the installed ESS and conventional and renewable DGs in the MGG distribution system are summarized in Table 3, Table 4, and Table 5, respectively.

The costs associated with DG generation, ESS charging and discharging, load shifting and shedding, as well as power transactions between microgrids, are shown Table 6, in per unit of cost for generation of conventional DGs.

## V. NUMERICAL SIMULATIONS

In the following sections, two test case scenario simulations are presented. In the first scenario, the MGG test system is

**TABLE 3.** Technical specifications of ESS units.

<b>s</b>	<b>i</b>	<b>C<sub>s,i</sub><sup>ESS</sup> [kWh]</b>	<b>P<sub>g,i</sub><sup>DCh/Ch,ma</sup> [kW]</b>	<b>η<sub>s,i</sub><sup>ch</sup></b>	<b>η<sub>s,i</sub><sup>dch</sup></b>	<b>SOC<sub>s,i</sub><sup>min</sup></b>	<b>SOC<sub>s,i</sub><sup>max</sup></b>	<b>SOC<sub>s,i</sub><sup>max</sup></b>
1	1	520	26	0.95	0.95	20%	90%	70%
2	2	650	32.5	0.95	0.95	20%	90%	70%
3	3	780	40	0.97	0.95	20%	90%	70%

**TABLE 4.** Technical specifications of DG units.

<b>g</b>	<b>i</b>	<b>P<sub>g,i</sub><sup>CG,max</sup> [kW]</b>	<b>P<sub>g,i</sub><sup>CG,min</sup> [kW]</b>	<b>UT<sub>g,i</sub> [hour]</b>	<b>DT<sub>g,i</sub> [hour]</b>	<b>UR<sub>g,i</sub> [kW]</b>	<b>DR<sub>g,i</sub> [kW]</b>
1	1	350	28	1	2	50	50
2	2	150	25	1	1	50	50
3	3	70	7	1	1	40	40

**TABLE 5.** Maximum Generation Capacity of PV Generation and Wind Generation Systems In Each Microgrid.

<b>r</b>	<b>Type</b>		<b>i</b>	<b>P<sub>r,i</sub><sup>RG,max</sup> [kW]</b>
1	PV generation System		1	20
2	Wind generation system			15
3	PV generation System		2	200
4	Wind generation system			80
5	PV generation System			50
6	Wind generation system		3	300

**TABLE 6.** Costs associated with local and global optimization problems.

<b>C<sup>CG</sup></b>	<b>C<sup>PV</sup></b>	<b>C<sup>Wind</sup></b>	<b>C<sup>Ch</sup></b>	<b>C<sup>Dch</sup></b>	<b>C<sup>Shed,Lp</sup></b>	<b>C<sup>Shed,MP</sup></b>	<b>C<sup>Shed,HP</sup></b>	<b>C<sup>Shift</sup></b>	<b>C<sup>Trans</sup></b>
1	0.3	0.5	0	0.8	5	10	15	0	1.4

assumed to be islanded from the utility grid for eight consecutive hours. In addition, each tie line is assumed to have 50 kW capacity, the local scheduling horizon ( $T_{local}$ ) of microgrids is set to three hours, and 5% of the hourly demand is assumed to be shiftable. The second test case scenario is similar to the first, but aims to simulate more severe conditions. Thus, it is assumed that conventional DG in Microgrid-1 is unavailable in the last two hours of the outage and Microgrid-2 is isolated from the rest of the system for two hours at the beginning of the emergency period.

In each scenario, 24 outages spanning eight hours with different starting times are simulated. In each outage simulation, the unsupplied energy for both autonomous and cooperative (applying the restoration technique) MGG system operation is calculated and the SI reflecting the enhancements attained by applying the proposed technique is determined. Since the main objective of this study is to balance the power locally and globally in the system during islanded operation, all the system parameters are assumed to be within the power flow constraints limits.

## A. SCENARIO I (THREE RESIDENTIAL MICROGRIDS)

Initially, each of the microgrids was set to operate independently and was disconnected from the main utility grid. The total curtailed energy for the three microgrids during the emergency for different emergency starting times is presented in Table 7. Each entry represents the MGG distribution system unsupplied energy during an outage that lasted eight

**TABLE 7.** Total unsupplied energy (Scenario I).

Emergency Starting Time (h)	Total Unsupplied Energy (kWh)	
	Autonomous Mode	Collaborative Mode
0	805	320
1	600	80
2	440	20
3	380	0
4	370	0
5	365	0
6	350	15
7	360	0
8	350	0
9	360	0
10	360	0
11	370	5
12	380	0
13	380	4
14	370	25
15	420	20
16	700	200
17	900	390
18	1,050	470
19	1,120	480
20	1,170	500
21	1,160	540
22	1,165	560
23	1,020	450

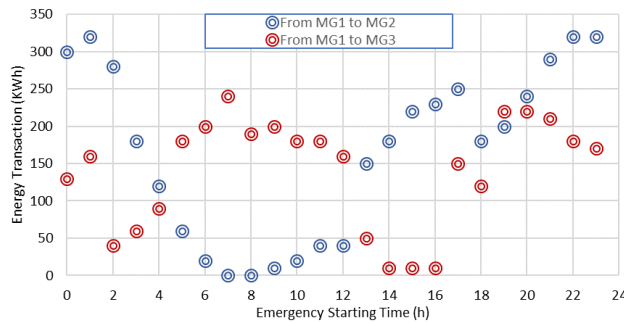


**FIGURE 6.** Scenario I: Total energy transactions from Microgrid-1 vs emergency starting time.

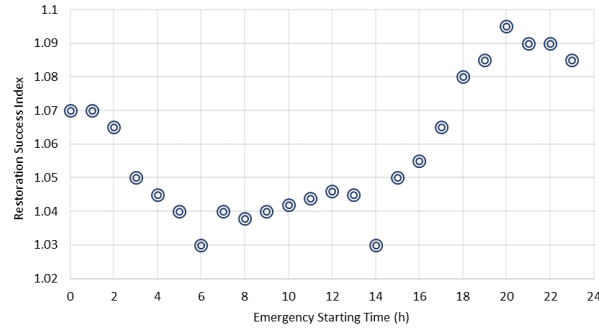


**FIGURE 7.** Scenario I: Load restoration technique success index (SI).

hours and started at a certain time. Next, the load restoration technique was applied and the microgrids were made to cooperate with each other. The resulting total unsupplied energy for different emergency starting times is also shown in Table 7.

The simulation findings indicate that the total amount of energy curtailment for all emergency starting times decreased, especially when the emergency occurred during the day. This was expected, as Microgrid-1 was able to supply its load because it had a capacity of dispatchable generation that covered its demand. Consequently, Microgrid-1 had sufficient flexibility to support other microgrids. In addition, Microgrid-2 had a relatively high capacity for the solar generation system, which peaks during the day hours, and could thus share surplus energy during these periods. The total energy transactions from Microgrid-1 to Microgrid-2 and Microgrid-3 for different emergency starting times are shown in Figure 6.

Finally, SI was calculated for all considered emergency starting times, as shown in Figure 7, and the average was found to be around 1.0567. Thus the ability of the proposed restoration technique to enhance the overall system performance was confirmed, as it was superior to the results obtained in the scenario in which microgrids operated autonomously. This was indicated by  $SI > 1$ . Finally, it can be concluded that, by applying the proposed technique, the overall load restoration performance was improved by  $>50\%$ .

**TABLE 8.** Total unsupplied energy (Scenario II).

Emergency Starting Time (h)	Total Unsupplied Energy (kWh)	
	Autonomous Mode	Collaborative Mode
0	1,300	840
1	1,100	640
2	950	610
3	850	600
4	850	605
5	850	600
6	800	600
7	900	620
8	850	470
9	900	420
10	920	460
11	940	600
12	960	610
13	960	620
14	940	600
15	1,000	640
16	1,250	850
17	1,350	1,100
18	1,500	1,200
19	1,600	1,220
20	1,600	1,220
21	1,550	1,200
22	1,500	1,200
23	1,500	1,050

## B. SCENARIO II (MORE SEVERE CONDITIONS)

Akin to Scenario I, microgrids were initially set to supply only their local loads and operated autonomously. The total load curtailment for all possible emergency starting times is represented in Table 8. Compared to Scenario I, the amount of unsupplied energy increased dramatically for all considered emergency starting times. This increase arises due to the Microgrid-1 dependency on the installed conventional DG, which was assumed to be out of service for two hours during the emergency. Again, to facilitate comparison, the unsupplied energy for emergencies with all possible starting times after applying the proposed restoration technique was calculated and is shown in Table 8.

Compared to the cooperative microgrid operation simulated in Scenario I, in this case, the total unsupplied energy for almost all emergency starting times increased. This increase is reasonable, as the MMG distribution system was subjected to more severe conditions. It can be deduced from the histogram shown in Table 8 that the increase in unsupplied energy was particularly pronounced for emergencies that occurred during the day. This was due to the disconnection of Microgrid-3 from the other microgrids. Microgrid-3 normally depends on the energy transactions from Microgrid-1 and Microgrid-2 during daytime emergencies due to its low local generation capacity. This dependency was compromised in Scenario II, resulting in the observed increase in the unsupplied energy. The total energy transactions from

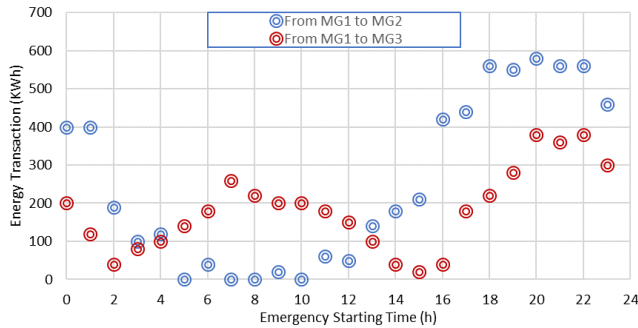


**FIGURE 8.** Scenario II: Total energy transactions from Microgrid-1 vs emergency starting time.

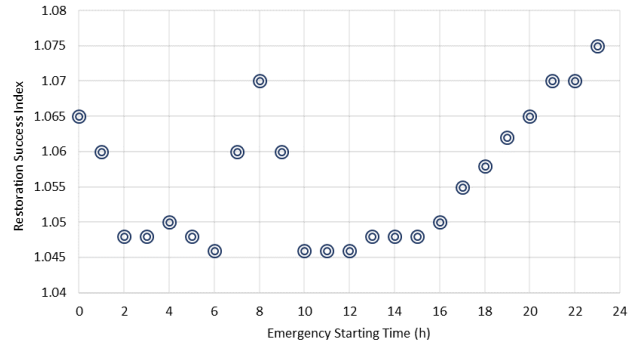


**FIGURE 9.** Scenario II: Load restoration technique Success Index (SI).

Microgrid-1 to Microgrid-2 and Microgrid-3 for different emergency starting times are shown in Figure 8.

Even though the system was subjected to more severe emergencies, the proposed technique enhanced the overall performance and exhibited satisfactory performance. To support this assertion, the load restoration technique SI was calculated for emergencies with all possible starting times, as shown in Figure 9. The maximum restoration success index was calculated at 1.0697, with the mean of 1.0546.

## VI. CONCLUSION

In this work, a novel outage management strategy of interconnected microgrids during islanded operation, particularly after being disconnected from the utility main supply, has been addressed based on the two-stage load restoration. The strategy was tested on a multi microgrid distribution system with the sole objective of restoring the maximum number of disconnected loads. The complex optimization problem was solved by adopting a well-known mixed integer linear programming technique. The performance of the proposed technique was reflected in the novel success index, which was specifically developed for this purpose. Sensitivity analysis was performed to study the impact of incorporating preemptive load shifting DR program. The DR program was found to enhance the overall system performance. However, a significant amount of load shifting caused performance degradation for the proposed technique. The proposed methodology is, however, quite general and can be easily applied to other types of distribution systems.

## REFERENCES

- [1] S. Ramchurn, P. Vytelingum, A. Rogers, and N. Jennings, “Putting the ‘smarts’ into the smart grid: A grand challenge for artificial intelligence,” *Commun. ACM*, vol. 55, no. 4, pp. 86–97, 2012.
- [2] A. Kenward and U. Raja. (Apr. 2014). *Blackout: Extreme Weather, Climate Change And Power Outages*. Accessed: May 2019. [Online]. Available: <http://www.ourenergypolicy.org/wp-content/uploads/2014/04/climate-central.pdf>
- [3] *Economic Benefits of Increasing Electric Grid Resilience to Weather Outages*, Executive Office President, IEEE USA Books & eBooks, Washington, DC, USA, 2013.
- [4] *Climate Change: Energy Infrastructure Risks and Adaptation Efforts*, Dept. Energy, U.S. Government Accountability Office, Washington, DC, USA, Jan. 2014.
- [5] *Enhancing Distribution Resiliency: Opportunities for Applying Innovative Technologies*, Electr. Power Res. Inst. (EPRI), Palo Alto, CA, USA, 2013.
- [6] K. P. Schneider, F. K. Tuffner, M. A. Elizondo, C.-C. Liu, Y. Xu, and D. Ton, “Evaluating the feasibility to use microgrids as a resiliency resource,” *IEEE Trans. Smart Grid*, vol. 8, no. 2, pp. 687–696, Mar. 2017.
- [7] H. Jia, X. Jin, Y. Mu, and X. Yu, “A multi-level service restoration strategy of distribution network considering microgrids and electric vehicles,” in *Proc. Int. Conf. Intell. Green Building Smart Grid (IGBSG)*, Taipei, Taiwan, Apr. 2014, pp. 1–4.
- [8] Y. Xu, C.-C. Liu, K. P. Schneider, F. K. Tuffner, and D. T. Ton, “Microgrids for service restoration to critical load in a resilient distribution system,” *IEEE Trans. Smart Grid*, vol. 9, no. 1, pp. 426–437, Jan. 2018.
- [9] C. Gouveia, J. Moreira, C. L. Moreira, and J. A. P. Lopes, “Coordinating storage and demand response for microgrid emergency operation,” *IEEE Trans. Smart Grid*, vol. 4, no. 4, pp. 1898–1908, Dec. 2013.
- [10] A. Khodaei, “Resiliency-oriented microgrid optimal scheduling,” *IEEE Trans. Smart Grid*, vol. 5, no. 4, pp. 1584–1591, Jul. 2014.
- [11] S. Bessler, D. Hovie, and O. Jung, “Outage response in microgrids using demand side management,” in *Proc. IEEE Int. Smart Cities Conf. (ISC2)*, Trento, Italy, Sep. 2016, pp. 1–6.
- [12] K. Balasubramaniam, P. Saraf, R. Hadidi, and E. B. Makram, “Energy management system for enhanced resiliency of microgrids during islanded operation,” *Electr. Power Syst. Res.*, vol. 137, pp. 133–141, Aug. 2016.
- [13] *IEEE Guide for Design, Operation, and Integration of Distributed Resource Island Systems With Electric Power Systems*, IEEE Standard 1547.4-2011, Jul. 2011, pp. 1–54.
- [14] M. Goyal and A. Ghosh, “Microgrids interconnection to support mutually during any contingency,” *Sustain. Energy, Grids Netw.*, vol. 6, pp. 100–108, Jun. 2016.
- [15] Z. Wang, B. Chen, J. Wang, and C. Chen, “Networked microgrids for self-healing power systems,” *IEEE Trans. Smart Grid*, vol. 7, no. 1, pp. 310–319, Jan. 2016.
- [16] A. Hussain, V.-H. Bui, and H.-M. Kim, “A resilient and privacy-preserving energy management strategy for networked microgrids,” *IEEE Trans. Smart Grid*, vol. 9, no. 3, pp. 2127–2139, May 2018.
- [17] M. Zadsar, M. Haghifam, and S. M. M. Larimi, “Approach for self-healing resilient operation of active distribution network with microgrid,” *IET Gener., Transmiss. Distrib.*, vol. 11, no. 18, pp. 4633–4643, Dec. 2017.
- [18] A. Arif and Z. Wang, “Networked microgrids for service restoration in resilient distribution systems,” *IET Gener., Transmiss. Distrib.*, vol. 11, no. 14, pp. 3612–3619, Sep. 2017.
- [19] A. Hussain, V.-H. Bui, and H.-M. Kim, “Optimal operation of hybrid microgrids for enhancing resiliency considering feasible islanding and survivability,” *IET Renew. Power Gener.*, vol. 11, no. 6, pp. 846–857, May 2017.
- [20] C. Chen, J. Wang, F. Qiu, and D. Zhao, “Resilient distribution system by microgrids formation after natural disasters,” *IEEE Trans. Smart Grid*, vol. 7, no. 2, pp. 958–966, Mar. 2016.
- [21] CPLEX. (2017). *IMM-ILOG*. [Online]. Available: <https://CPLEX.com>
- [22] *MLU Series Photovoltaic Modules, PV-MLU255HC, Datasheet*, Mitsubishi Electric, Tokyo, Japan, Mar. 2012.
- [23] *3.5 kW Wind Turbine System, Datasheet*, Raum Energy, Saskatoon, SK, Canada.

**MOHEEB OTT** received the B.Sc. and M.Sc. degrees in electrical engineering from the King Fahd University of Petroleum and Minerals (KFUPM), Dhahran, Saudi Arabia, in 2015 and 2018, respectively. His research interests include power system operation and planning, smart grids and microgrids, and renewable energy resources.



**MOHAMMAD ALMUHAINI** received the B.Sc. and M.Sc. degrees in electrical engineering from the King Fahd University of Petroleum and Minerals (KFUPM), Saudi Arabia, in 2004 and 2007, respectively, and the Ph.D. degree from Arizona State University (ASU), Tempe, US, in 2012. He is currently an Assistant Professor with the Electrical Engineering Department, King Fahd University of Petroleum and Minerals (KFUPM). His research interests include evaluating the reliability of power distribution systems, Markov model applications in power systems, and smart grids and secondary distribution networks.



**MUHAMMAD KHALID** received the Ph.D. degree in electrical engineering from the School of Electrical Engineering & Telecommunications (EE&T), University of New South Wales (UNSW), Sydney, Australia, in 2011. He was a Postdoctoral Research Fellow with UNSW for three years and a Senior Research Associate with the School of EE&T, Australian Energy Research Institute, UNSW, for two years. He is currently an Assistant Professor with the Electrical Engineering Department, King Fahd University of Petroleum and Minerals (KFUPM), Dhahran, Saudi Arabia. He is also a Researcher with K.A.CARE Energy Research and Innovation Center, Dhahran. He has authored/coauthored several journal and conference papers in the field of control and optimization for renewable power systems. His current research interests include optimization and control of battery energy storage systems for large-scale grid-connected renewable power plants (particularly wind and solar), distributed power generation and dispatch, hybrid energy storage, EVs, and smart grids. In 2010, he received a highly competitive postdoctoral writing fellowship from UNSW. Most recently, he has received a prestigious K.A.CARE fellowship. He has served as a reviewer for numerous international journals and conferences.

• • •